Major Comments
The authors have put considerable effort into answering both referees' queries and the manuscript is much improved over the previous version. However the explanation of the processes generating the polynya is still not quite convincing and needs further work. Certainly plots of salinity need to be presented in Fig. 2, as well as those of temperature and density.

We thank the reviewer for having agreed to review this second version of the manuscript and for their new comments, in particular for spotting a critical inconsistency between one figure and our analysis. We have corrected our text accordingly, highlighting the key role played by salinity in this new analysis, and hence have added the salinity plots. However, for better readability, these are not presented on Fig. 2 as suggested but rather on a new figure, along with the plots for temperature and density. See the detailed answer for each point below.

A naive view of Antarctic open-ocean polynya formation is that it is fundamentally a consequence of extra salinity in the surface waters that permits the water to get dense enough to convect while it is still above freezing. Once the convection `punches through' into the warm salty upper circumpolar deep waters, then it continues bringing up salt and the convection penetrates very deeply and can be sustained for several winters. The warm water in the polynya is the consequence of heat being brought up from below. Therefore consideration of the evolution of the salinity structure is essential to understand the process of polynya generation. This is still missing from the MS.

We agree with the reviewer that the role of salinity must not be forgotten in our analysis, in particular now that we have modified the beginning of the explanation of the triggering mechanism in the control run following the reviewer's point ii (see below). Nevertheless we would like to point out that the physics of the real ocean and the parameterisations of ocean models do not always agree. Here for example warm waters are not only a consequence of the polynya, with heat being brought from below, but also a cause for the formation of said polynya. Even if these waters are not key for initiating deep convection, the fact that they are well above freezing when sea ice should form does result in a polynya. Hence, rather than modifying the manuscript to show the dominant role of salinity in triggering deep convection, we have rewritten it to show the importance of both temperature and salinity. See for example p9:

the decrease in winds.With a reduced mixed layer entrainment, a warm and salty anomaly develops below the mixed layer ($1.5\,^\circ$C and 0.25 in September 1985, Fig. 3a and c). When ice-free in summer, the warm salty waters are incorporated in the mixed layer, which is no longer anomalously shallow (deepening from $48\,$m in January 1986 to $120\,$m in May). The surface waters become anomalously warm (Fig. 3a), remaining above the freezing point until June 1986 (Fig. 3b). The warm surface waters impede sea ice formation, resulting in the development of an open ocean polynya over August to October 1986 (maximum extent of $22\,000\,$km^2 in September 1986, Fig. 2c), north of the 1987 polynya. These surface waters are also strongly anomalously salty and hence dense from June 1986 (Fig. 3c and e), and become even more so once the polynya is open. In agreement with observations

It seems to me from the evolution of density in Fig. 2h that a key driver of the model polynya is the very salty (because it's warm but anomalously dense) water lying at depths of 50-100m in 1985-1986 that becomes entrained into the ML in autumn 1986. But this would be clear if you plotted the salinity evolution.

Following the reviewer's suggestion, Fig. 3 now presents the evolution of temperature and density as well as salinity, with time and depth. We agree with the reviewer that one of the key drivers of the deep convection event of 1987 is the fact that this warm and salty water mass is brought up from 50 m to the surface by the deep mixed layers of 1986, as is mentioned in the text and now shown on Fig.3c and d:

conditioning the ocean for deep convection. In October 1986, the isopycnals are vertical (Fig. 3f) and the surface waters are anomalously dense (Fig. 3e) because of the brine rejection in the polynya and because deep salty waters have been brought up by convection (Fig. 3d). Moreover, the increased convection reaches the layer of relatively warm waters, which enhance the warm anomaly at the surface (from January 1987, Fig. 3a) so that again the ocean surface is above freezing temperature when the sea ice should grow (Fig. 3b). Meanwhile, not only are the surface waters anomalously saline and dense because of brine rejection in winter, they also remain anomalously saline and dense through spring and summer (Fig. 3 c and e), as no ice is available to be melted at the location of the polynya. As

(i) The inclusion of the water-column trajectory in Fig. 2e is very useful. However, this trajectory starts only in August 1986 (unless it didn't move from March 1985-August-1986, in which case it needs to be made clearer). So where does the data come from that is used in the Hovmöller diagrams 2f-i before August 1986?

We apologise for the confusion regarding the Hovmöller diagrams. Some of the key information was lost when we introduced the plot of the trajectory. The Hovmöller diagrams are averaged over the following areas:
- until August 1986, the area of the 1986 polynya (dashed black contours on Fig. 2e)
- from September 1986 to June 1987, the trajectory shown on Fig. 2e
- from July 1987, the area of the 1987 polynya (plain black contours on Fig. 2e)

It is now explicitly written in the caption of Fig. 3:

Figure 3. Hovmoller diagrams, as a function of depth and time, of properties averaged over the area of the 1986 polynya (dashed black contour on Fig. 2e) until August 1986, along the trajectory of Fig. 2e from September 1986 to June 1987, and over the area of the 1987 polynya (plain black contour on Fig. 2e) from July 1987: a) potential temperature anomalies (relative to Jan. 1980 to Dec.

(ii) Some of the text on p9 seems inconsistent with the revised argument. In para 2, l3 the text mentions 'ice fraction increased by more than 0.2', in June 1985, but at 63 deg S, near the 1986 polynya, which is presumably where the trajectory is at this stage (comment(i)), the ice fraction anomaly is actually negative according to Fig. 2a. Similarly Fig. 2b suggests that the MLD anomaly is only ≈10m (or even not significant) there.

We sincerely thank the reviewer for pointing out this strong inconsistency in our manuscript. It is true that although we study the triggers for the large deep convection event (black contours on Fig. 2), we first need to focus on the anomalies that occur at the location of the 1986 polynya, around 63°S (now represented by dashed black contours on Fig. 2a and b). The reviewer is right that the text needs to be modified: here there is a negative sea ice anomaly, not positive, and a warm and salty anomaly in the surface waters. This result is consistent with the findings of Kjellsson et al. (2015), who showed the role of sea ice deficit in triggering Southern Ocean deep convection in NEMO3.6. We have modified the text as follows:

The process leading to deep convection starts two years earlier with a decrease of the katabatic winds off the Antarctic coast. It results in a positive and significant sea ice area anomaly in June 1985 close to the coast, and a negative anomaly further offshore (probably due to a lack of sea ice export) where the first polynya will open (more than 0.2, dashed black contours on Fig. 2a). In agreement with Kjellsson et al. (2015), we find that the sea ice deficit is associated with a warm and salty anomaly of the top 50 m (Fig. 3a and c). Meanwhile, the MLD is anomalously shallow (Fig. 2b), which could be a consequence of the decrease in winds. With a reduced mixed layer entrainment, a warm and salty anomaly develops below the mixed layer ($1.5\,^{\circ}C$ and 0.25 in September 1985, Fig. 3a and c). When

(iii) p9, para 2, 3rd line from last. You state that `the model polynya allows the formation of dense water at the surface due to brine rejection'. You need to justify this in terms of something like ice divergence,because the naive expectation is that in a polynya, where there's no ice, there can be no brine rejection.

We are not sure that we understand the reviewer's point. It is an accepted result (e.g. Comiso 2010 for a review of the literature on polynyas) that although polynyas are ice-free, extensive sea ice formation occurs in them due to the large temperature gradient between Antarctic winter atmosphere and the relatively warm ocean. Hence there is brine rejection at the surface of the polynya.

(iv) Surface waters will not follow the column trajectory because they are influenced by the Ekman drift. You might want to consider what impact this has on the salt budget of the column.

We had shown as a response to the reviewer's comment on the previous version of the manuscript that the flow of the top 300 m is quasi barotropic (at least when considering our monthly mean output).

Minor Comments

p9, Section 3.1 title. Better would be 'Mechanism of polynya formation in the control run'

Polynya formation is not the topic of the manuscript, we talk a lot about polynya only because in this model it is associated with open ocean deep convection. We have however modified the title so that it is clearer:

3.1   Mechanisms for triggering open ocean deep convection in the control run

p11, para 3. 'The warmer the ocean is in summer and autumn 1986, the less sea ice can form, so the larger the polynya in winter 1986'. I just don't think it's that simple-as I stated in my previous review-warmer summer ML by itself will just slightly delay the formation of ice the next winter. Enhanced salinity is required.

The reviewer is right that the actual detailed mechanism is not as simple as stated in that sentence. In addition to the reference of Heuzé (2015) in the introduction, we have now added the following sentence to mention the "salt-enhancement loop":

linear and significant, albeit with some uncertainty in the surface properties. Note that the whole process is enhanced by salinity anomalies, in particular the larger the polynya, the saltier the surface waters and the more destabilised the water column (Heuzé, 2015).

Major changes to the manuscript:
- addition of a new figure 3, containing panels f to i of Fig. 2 of the previous version of the manuscript, as well as the salinity plots required by the reviewer and the editor.
- Figs. 3 to 6 of the previous version of the manuscript are now Figs. 4 to 7.
- Fig. 2a and b, black dashed contours at the location of the 1986 polynya
- addition of the reference to Kjellsson et al. (2015):
  Kjellsson, J, Holland, P. R., Marshall, G. J., Mathiot, P., Aksenov, Y., Coward, A. C., Bacon, S., Megann, A. P., and Ridley, J. K.: Model sensitivity of the Weddell and Ross seas, Antarctica, to vertical mixing and freshwater forcing, Ocean Model., 94, 141–152, doi:10.1016/j.ocemod.2015.08.003, 2015.
- text changes are in red in the manuscript

Increasing vertical mixing to reduce Southern Ocean deep convection in NEMO3.4

C. Heuzé[1,2,*]**, J. K. Ridley**[2]**, D. Calvert**[2]**, D. P. Stevens**[1]**, and K. J. Heywood**[1]

[1]Centre for Ocean and Atmospheric Sciences, University of East Anglia, Norwich, NR4 7TJ, UK
[2]Met Office, Hadley Centre, Exeter, EX1 3PB, UK
[*]now at Department of Marine Sciences, University of Gothenburg, 405 30, Sweden

Correspondence to: C. Heuzé (celine.heuze@gu.se)

Abstract

Most CMIP5 models unrealistically form Antarctic Bottom Water by open ocean deep convection in the Weddell and Ross Seas. To identify the mechanisms triggering Southern Ocean deep convection in models, we perform sensitivity experiments on the ocean model NEMO3.4 forced by prescribed atmospheric fluxes. We vary the vertical velocity scale of the Langmuir turbulence, the fraction of turbulent kinetic energy transferred below the mixed layer, and the background diffusivity and run short simulations from 1980. All experiments exhibit deep convection in the Riiser-Larsen Sea in 1987; the origin is a positive sea ice anomaly in 1985, causing a shallow anomaly in mixed layer depth, hence anomalously warm surface waters and subsequent polynya opening. Modifying the vertical mixing impacts both the climatological state and the associated surface anomalies. The experiments with enhanced mixing exhibit colder surface waters and reduced deep convection. The experiments with decreased mixing give warmer surface waters, open larger polynyas causing more saline surface waters and have deep convection across the Weddell Sea until the simulations end. Extended experiments reveal an increase in the Drake Passage transport of 4 Sv each year deep convection occurs, leading to an unrealistically large transport at the end of the simulation. North Atlantic deep convection is not significantly affected by the changes in mixing parameters. As new climate model overflow parameterisations are developed to form Antarctic Bottom Water more realistically, we argue that models would benefit from stopping Southern Ocean deep convection, for example by increasing their vertical mixing.

1 Introduction

Full depth open ocean deep convection has been observed only once in the Southern Ocean, during the Weddell Polynya of 1974-1976 (Gordon, 1978). Otherwise, the mixed layer depth in the southern subpolar gyres does not exceed 1000 m (Schmidtko et al., 2013). In state-of-the-art CMIP5 models, Antarctic Bottom Water (AABW) is formed via

2

open ocean deep convection (deeper than 2000 m and up to full-depth) which occurs most winters in the seasonally ice covered southern subpolar gyres (Heuzé et al., 2013) and continues throughout climate change simulations (Heuzé et al., 2015). Not only is this process relatively unrealistic, it also leads to spurious ocean properties, variabilities and drift (e.g. Latif et al., 2013; Megann et al., 2014) and can render reanalyses useless (Azaneu et al., 2014). Martin et al. (2013) and Cheon et al. (2014) have shown that each event of open ocean deep convection accelerates the southern subpolar gyres and hence increases the Antarctic Circumpolar Current (ACC) transport to unrealistically high values. With the advent of new methods to form and export AABW more realistically (e.g. Briegleb et al., 2010; Bates et al., 2012; Adcroft, 2013), it would be desirable to eliminate unrealistic Southern Ocean deep convection.

Here we investigate the role of ocean model parameterisations in triggering open ocean deep convection in the Southern Ocean. Observations and models alike show that a preconditioning mechanism, reducing the static stability of the water column, is necessary before deep convection can commence (Martinson et al., 1981). According to Losch et al. (2006), static instability arises because the current generation of ocean models mixes vertically too weakly when given heterogeneous surface conditions. Buoyancy loss and mixing imposed by sea ice concentration less than unity are averaged over the horizontal grid; with weak mixing, the stratification becomes unstable. Wind-induced mixing determines the amount of turbulent kinetic energy (TKE) penetrating the mixed layer, which if underestimated can result in a disconnection between the surface and the rest of the water column, leading to a surface salt accumulation and subsequent loss of static stability (Timmermann and Beckmann, 2004). More recently, Calvert and Siddorn (2013) and Megann et al. (2014) have demonstrated the sensitivity of high latitude mixed layers to vertical mixing. All these studies suggest that vertical mixing needs to be increased to reduce deep convection in models.

The ocean model NEMO3.4 (Madec, 2008) is used here in its configuration ORCA025 (nominal horizontal resolution of $0.25°$, 75 vertical levels) and is coupled to the CICE sea ice model (Hunke and Lipscomb, 2008). It will be hereafter referred to only as NEMO.

Vertical mixing of momentum and tracers is treated using a TKE scheme (Gaspar et al., 1990), with convection being parameterised by an enhancement of the calculated vertical eddy diffusivity and viscosity. The ocean is forced with a prescribed atmospheric forcing from CORE2 (Large and Yeager, 2009). The ocean model configuration used in this study exhibits deep convection in the Weddell Sea (Megann et al., 2014).

Here we investigate the role of vertical mixing parameterisations on Southern Ocean deep convection with sensitivity experiments on NEMO3.4. We detail these experiments in Sect. 2, along with our methods. In Sect. 3, we briefly explain the mechanism triggering deep convection in the control experiment before showing how this mechanism is modified in the sensitivity experiments. Note that longer, more detailed explanations of these results are given by Heuzé (2015). We also study the impact of the changes of parameter on the ACC and North Atlantic deep convection in Sect. 3. Our results are summarised and discussed, along with their limitations, in Sect. 4.

2 Sensitivity experiments and methods

2.1 Parameters studied

The purpose of these experiments is to identify a method to reduce the occurrence of open ocean deep convection in the NEMO Southern Ocean. The experiments are based on similar work performed by Calvert and Siddorn (2013) who varied 13 parameters of the TKE scheme and studied their impact on the shallow bias in the Southern Ocean summer mixed layer depth. Note that their experiments were performed with a different ocean resolution (1° compared with 0.25° here). Their findings established which values to use in the most recent joint NERC-Met Office configuration of the ocean model, "GO5" (Megann et al., 2014), which provide the base settings used in our experiments. Our "Control" experiment is the GO5 run "amhih" (see Code availability at the end of this manuscript). Following the findings of Calvert and Siddorn (2013) and Megann et al. (2014), we increase and decrease just three parameters as detailed below. The background diffusivity experiments extend

throughout the entire period of available CORE2 atmospheric forcing (27 years, 1980 to 2006) while the other experiments have run for 10 years (1980-1989). All the experiments are summarised in Table 1.

2.1.1 Langmuir turbulence velocity scale "c_{LC}"

Langmuir turbulence is represented in NEMO by the parameterization of Axell (2002), which appears as an additional production term in the TKE budget equation:

$$\frac{d\overline{e}}{dt} = \frac{W^3}{L}, \tag{1}$$

where W is a velocity scale, taken to be the maximum downwelling velocity of the Langmuir cell and L is a length scale, taken to be the vertical extent of the cell. A sinusoidal profile is assumed for the cell so that:

$$W = cV_{10} = c_{LC}V_s|_{z=0}\sin\left(-\frac{\Pi z}{L}\right) \quad \text{for} -z \leq L,$$

$$W = 0 \quad \text{for} -z > L, \tag{2}$$

where $V_s|_{z=0} = 0.016V_{10}$ is the surface value of the Stokes drift for a fully-developed sea (Li and Garrett, 1993), V_{10} is the 10 m wind speed and c_{LC} is a scaling coefficient, suggested by Axell (2002) to be between 0.15 and 0.2 based on a comparison with Large Eddy Simulation results.

Averaging over 1982–1985 and between 60–45° S in the Southern Ocean (i.e. north of the deep convection regions), Calvert and Siddorn (2013) show that increasing c_{LC} deepens the mixed layer throughout the year, decreasing the summer-autumn shallow bias but increasing the winter-spring deep bias. Here we test three cases:

– Langmuir turbulence parameterisation turned off ("LangmuirD")

– $c_{LC} = 0.15$: control experiment ("Control")

– $c_{LC} = 0.20$: case with increased vertical velocity scale ("LangmuirI").

2.1.2 Near-inertial wave breaking TKE scaling "γ"

NEMO features an ad-hoc parameterisation of the mixing due to the breaking of near-inertial waves excited by high-frequency winds, $\bar{e}_{\text{inertial}}$, which is added to the time-integrated TKE (Rodgers et al., 2014):

$$\bar{e}(t + \Delta t, z) = \int\limits_{t}^{t+\Delta t} \left(\frac{\partial \bar{e}}{\partial t}(z) \right) + \bar{e}_{inertial}(t, z). \tag{3}$$

$\bar{e}_{\text{inertial}}$ is defined as:

$$\bar{e}_{\text{inertial}}(t, z) = \gamma \bar{e}|_{z=0} \exp^{z/\lambda}, \tag{4}$$

where λ is an exponential decay scale, set as 10 m globally in the GO5 configuration, and γ is the parameter varied here (fraction of TKE penetrating below the mixed layer).

Calvert and Siddorn (2013) tested values of γ ranging from 0.005 to 0.095 (default 0.05). Considering the zonal average of the Southern Ocean between 60–45° S only, mixed layer depth biases decrease in NEMO in summer and winter as γ increases. As for c_{LC}, these averages do not include the Southern Ocean deep convection areas. The value of γ for the real ocean is unknown, hence the range of values suggested by Madec (2008) is purely numerical. In addition to the control, we consider only the two most extreme values:

- **–** $\gamma = 0.005$: case with decreased extra TKE mixing ("GammaD")

- **–** $\gamma = 0.050$: control experiment ("Control")

- **–** $\gamma = 0.095$: case with increased extra TKE mixing ("GammaI").

2.1.3 Background diffusivity profile and surface value

Unresolved and otherwise unparameterised vertical mixing processes are represented by a background vertical eddy diffusivity. In sensitivity experiments on ORCA025 (i.e. the same

resolution of NEMO as used here), Megann et al. (2014) increased the background diffusivity (constant through depth) from 1.0×10^{-5} to 1.2×10^{-5} m^2 s^{-1} and found a significant surface freshening and increased stratification in the Arctic. They did not detail their results for the Southern Ocean.

In NEMO, it is also possible to change the shape of the background diffusivity profile. Two shapes are implemented: the background diffusivity can either be constant through depth, or increase linearly with depth (diffusivity reaches 10 times the surface value at 4000 m depth, Madec, 2008). Unpublished experiments with HiGEM (Shaffrey et al., 2009), whose ocean model is not NEMO, suggest that the open ocean deep convection area is reduced in both southern subpolar gyres when the background diffusivity increases linearly instead of being constant with depth. Here we test the effects of modifying the vertical profile and/or the surface value of the background diffusivity:

– constant profile, surface diffusivity $= 1.0 \times 10^{-5}$ m^2 s^{-1} ("KnoprofD")

– constant profile, surface diffusivity $= 1.2 \times 10^{-5}$ m^2 s^{-1}, control experiment ("Control")

– linear profile, surface diffusivity $= 1.2 \times 10^{-5}$ m^2 s^{-1} ("Kprof")

– linear profile, surface diffusivity $= 1.3 \times 10^{-5}$ m^2 s^{-1} ("KprofI").

2.2 Methods

To assess the state of the ocean, we use the potential temperature (hereafter referred as temperature only), salinity, sea ice concentration and mixed layer depth (MLD) diagnostics from NEMO, in its configuration ORCA025 (horizontal resolution of $0.25°$) and with the GO5.0 default settings (Megann et al., 2014). We compute the potential density (hereafter referred as density only) relative to the surface σ_θ using the equation of state EOS80 (Fofonoff and Millard, 1983). The MLD is determined in the model using a density σ_θ threshold of 0.01 kg m^{-3} from the 10 m depth value (Madec, 2008). The observed global MLD was obtained from the climatology of Schmidtko et al. (2013). Following Heuzé et al. (2015), we consider that there is open ocean deep convection in the Southern Ocean (latitude south

of 50°S) if the local monthly mean MLD reaches at least 2000 m where the bathymetry is deeper than 3000 m. We compute the total area of deep convection as the sum of individual model grid cell areas where the MLD exceeds 2000 m.

We define an open ocean polynya as a region where the sea ice area fraction is locally less than 0.15, surrounded by a zone where the sea ice area fraction is greater than 0.15 (i.e. not directly connected to the ice-free ocean). Likewise, we compute the total polynya area as the sum of the areas of connected model grid cells where the criteria for a polynya are met. Anomalies are calculated relative to the first half of the simulation (January 1980 to December 1984), before the onset of deep convection. Anomalies are considered significant if they are larger than the monthly temporal standard deviation during 1980-1984. To account for the advection of the anomalies by the local currents (which have little vertical shear for the depth range studied and exhibit temporal variability, not shown), we define the trajectory between the first two polynyas (1986 and 1987) as the succession of monthly positions occupied by the water that was in the polynya in September 1986, inferred from the subsequent monthly horizontal velocity vectors.

To assess the impact of Southern Ocean deep convection on the large-scale circulation, we calculate the Antarctic Circumpolar Current volume transport as the annual total mean volume transport through Drake Passage. We integrate the zonal velocity from the Antarctic Peninsula to South America, and then over depth from the sea floor to the surface. The ACC volume transport is the total resulting from these integrations. Following for example Russell et al. (2006), we compare the ACC volume transport with the horizontal gradient in density across the ACC $d\rho$, defined as the zonally averaged density difference between 45° S and 65° S. We also check if the MLD in the North Atlantic is modified by our sensitivity experiments. We consider that there is deep convection in the North Atlantic (north of 50° N, 70° W to 20° E) if the local monthly mean MLD exceeds 1000 m (following observations by Våge et al., 2009, for example).

3 Results

3.1 Mechanisms for triggering open ocean deep convection in the control run

In order to assess how our parameter changes impact the model ocean, we first need to understand how model processes trigger Southern Ocean deep convection. In the control run, between 1980 and 1989, the maximum MLD exceeds 2000 m in the open ocean in the Riiser-Larsen Sea only (Fig. 1, blue box), in winter 1987.

The process leading to deep convection starts two years earlier with a decrease of the katabatic winds off the Antarctic coast. It results in a positive and significant sea ice area anomaly in June 1985 close to the coast, and a negative anomaly further offshore (probably due to a lack of sea ice export) where the first polynya will open (more than 0.2, dashed black contours on Fig. 2a). In agreement with Kjellsson et al. (2015), we find that the sea ice deficit is associated with a warm and salty anomaly of the top 50 m (Fig. 3a and c). Meanwhile, the MLD is anomalously shallow (Fig. 2b), which could be a consequence of the decrease in winds. With a reduced mixed layer entrainment, a warm and salty anomaly develops below the mixed layer ($1.5\,°$C and 0.25 in September 1985, Fig. 3a and c). When ice-free in summer, the warm salty waters are incorporated in the mixed layer, which is no longer anomalously shallow (deepening from 48 m in January 1986 to 120 m in May). The surface waters become anomalously warm (Fig. 3a), remaining above the freezing point until June 1986 (Fig. 3b). The warm surface waters impede sea ice formation, resulting in the development of an open ocean polynya over August to October 1986 (maximum extent of $22\,000\,\text{km}^2$ in September 1986, Fig. 2c), north of the 1987 polynya. These surface waters are also strongly anomalously salty and hence dense from June 1986 (Fig. 3c and e), and become even more so once the polynya is open. In agreement with observations (e.g. Killworth, 1979), the model polynya allows the formation of dense water at the surface (Fig. 3e and f) due to brine rejection, further destabilising the water column and inducing an increased salinity-driven convection that reaches a maximum depth of 827 m in September 1986 at the centre of the polynya.

The polynya and increased convection both act towards a decrease in stratification, pre-conditioning the ocean for deep convection. In October 1986, the isopycnals are vertical (Fig. 3f) and the surface waters are anomalously dense (Fig. 3e) because of the brine rejection in the polynya and because deep salty waters have been brought up by convection (Fig. 3d). Moreover, the increased convection reaches the layer of relatively warm waters, which enhance the warm anomaly at the surface (from January 1987, Fig. 3a) so that again the ocean surface is above freezing temperature when the sea ice should grow (Fig. 3b). Meanwhile, not only are the surface waters anomalously saline and dense because of brine rejection in winter, they also remain anomalously saline and dense through spring and summer (Fig. 3 c and e), as no ice is available to be melted at the location of the polynya. As the surface waters are anomalously warm, the polynya reopens in July 1987 and reaches a maximum extent of $68\,000\,\mathrm{km^2}$ in October 1987 (Fig. 2d). This polynya reopens further south than the one in 1986. That is because the warm and dense anomalies have been advected in a near-barotropic subsurface flow that brought them to the site of the 1987 polynya (Fig. 2e). Also, like real polynyas do (Smith and Barber, 2007), the 1986 model polynya and associated increased convection had an impact over a large area, lifting isopycnals significantly even at $66°\,\mathrm{S}$ where a lower than usual sea ice concentration can be seen (0.7 in the black contours of Fig. 2c).

The conjunction of weakly stratified waters and the second polynya results in open ocean deep convection from August to November 1987, reaching a maximum depth of 3200 m in October 1987. In the control run, deep convection does not restart in the subsequent years. As explained in the following section, surface waters are not warm enough to sustain deep convection after 1987. We shall now examine how the process triggering deep convection is modified in the parameter sensitivity experiments.

3.2 Modifications induced by the experiments

All sensitivity experiments start from the same initial conditions as the control simulation. Considering the mean 1980-1984 sea surface temperature, over the area that will convect (black contours on Fig. 2a), from November to March the decreased parameter experi-

ments (reduced vertical mixing) are warmer than the control. The increased parameter experiments (increased mixing) in contrast are colder than the control. The largest difference from the control is found in February, over the region of deep convection, for the TKE experiments: on average GammaD is warmer than the control by $0.34\,^{\circ}$C while GammaI is colder by $0.22\,^{\circ}$C. There is no significant difference in the winter sea surface temperature (SST), as the area is ice-covered and SST at the freezing point during 1980-1984 in all experiments. The winter mixed layer is modified by the Langmuir turbulence experiments ($5\,$m shallower than the control in LangmuirI, $5\,$m deeper in LangmuirD), but not significantly by the other experiments. This is consistent with the results of Calvert and Siddorn (2013): increasing the Langmuir turbulence velocity scale deepened their winter MLD by 5 to $10\,$m, whereas Gamma had little effect on it.

In winter 1985, all experiments show the same sea ice anomaly, at the same location, constrained by the atmospheric forcing. The temperature anomaly of summer 1986 differs significantly from that of the control run only for the Langmuir experiments (anomaly in LangmuirD warmer by $0.3\,^{\circ}$C than in the control and $0.1\,^{\circ}$C colder in LangmuirI) and for KnoprofD ($0.3\,^{\circ}$C warmer than the control). The results of the Langmuir experiments are consistent with those of Calvert and Siddorn (2013); the results of the background diffusivity experiments are more surprising as it is usually thought that the background diffusivity would not have any effect on such shallow MLD (e.g. Megann et al., 2014). The regional climatologies of the decreased parameter experiments are warmer than the control in the summer of 1986. Their vertical mixing is weaker than the control, and hence they accumulate warm and saline anomalies at the surface.

The warmer the ocean is in summer and autumn 1986, the less sea ice can form, so the larger the polynya in winter 1986 (Fig. 4a). The larger the polynya, the deeper and more extensive the convection of 1986 (Fig. 4b). The deeper the convection, the warmer the surface of the ocean after the convection (Fig. 4c), and consequently the larger the polynya in winter 1987 (Fig. 4d). The larger the 1987 polynya, the deeper the mixed layer and the larger the area of deep convection in 1987 (Figs. 4e and f). All relationships are relatively linear and significant, albeit with some uncertainty in the surface properties. Note that the

After 1987, the LangmuirD, GammaD, KnoprofD and Kprof keep convecting. This is not surprising: the positive feedback or "temperature loop" found above, sustained by warm water advection and brine rejection, has been responsible for decades of deep convection every winter in other models (e.g. Martin et al., 2013). As in other modelling studies (e.g. Martinson et al., 1981) the centre of the deep convection area is advected to the middle of the Weddell Gyre (Fig. 5). There is a very strong and significant across-run relationship between the deep convection area of 1987 in the Riiser-Larsen Sea and the area of the 1988 polynya and deep convection (correlation of 0.90). In fact, advected by a steady westward slope current, the warm anomalies induced by the 1987 deep convection in the Riiser-Larsen Sea propagate to the centre of the Weddell Gyre where deep convection occurs in 1988 and 1989 (Fig. 5 and 7a). The three increased parameter experiments (and the control) are not warm enough for their anomaly to trigger the opening of a polynya in 1988 (i.e. they do not have sufficient heat content to prevent sea ice formation), hence they stop convecting and their convection area is restricted to the Riiser-Larsen Sea (Fig. 5).

3.3 ACC and North Atlantic deep convection

We have focused on the impact of changes to the vertical mixing parameters on a specific ocean characteristic, the MLD. If these changes are to be considered part of the solution to spurious Southern Ocean deep convection, we must ensure that they have no adverse impact elsewhere in the global model ocean. We found that the ACC volume transport increases following deep convection in the Weddell Sea. Such a response had been hypothesised by Timmermann and Beckmann (2004). In an 18 year run of the model BRIOS2 with a specified atmospheric forcing, they found that Weddell Sea deep convection intensified the Weddell Gyre circulation, and suggested that it would then strengthen the ACC (theirs was prescribed). In agreement with other modelling studies (e.g. Russell et al., 2006; Meijers et al., 2012; Martin et al., 2015), deep convection in the Weddell Sea is associated with an increase in the horizontal density gradient, a key driver of the ACC (Fig. 6). We found a

significant correlation between the ACC volume transport and the area of deep convection (correlation of more than 0.6 for the three 27 year simulations, Fig. 6). For each year during which deep convection occurs, the ACC transport increases by 2 to 4 Sv.

We found an increase in the ACC tranport of nearly 25 Sv in the 27 year simulations. This result is consistent with the increase of more than 20 Sv found by Martin et al. (2013), and the increase of 20 % found by Cheon et al. (2014) while modelling the Weddell Polynya in GFDL-MOM4. Such an increase is an issue for the model, especially as in our experiments the atmospheric forcing is prescribed and does not react to deep convection. Even with a forced model, we obtain an unrealistically strong ACC: at the end of the run, all three long simulations have exceeded the observational range of 134–164 Sv (Griesel et al., 2012). These perturbed parameter experiments show that Southern Ocean deep convection disturbs the large scale oceanic circulation.

While deep convection in the Southern Ocean is a rather unrealistic process occurring in models, deep convection in the North Atlantic is a key driver of the global ocean circulation (e.g. Johnson, 2008). Ideally, we would like to minimalise Southern Ocean deep convection whilst maintaining North Atlantic deep convection. Our results suggest that this is possible (Fig. 7). Unlike in the Southern Ocean where a preconditioning is necessary (Fig. 7a), deep convection in the North Atlantic is persistent throughout the simulation (Fig. 7b), with differences between the experiments being less than the interannual variability. The differences due to parameterisations are not altered throughout the 27 year simulations, consistent with the findings of Megann et al. (2014); changing the background diffusivity has no significant effect on the northern high latitude MLD. In general, the GammaD and GammaI simulations have respectively the largest and smallest areas of deep convection; the other experiments show no consistency in the North Atlantic from 1980 to 1989 (Fig. 7b). Our results suggest that at least up to a decade, deep convection in the North Atlantic is not significantly modified by the three vertical mixing parameters found to have a large impact on the Southern Ocean deep convection. We obtain similar results when looking at the rest of the world ocean: outside of the deep convection regions (i.e. 60° S to 50° N, not shown), the year-long area-weighted mean difference in MLD between observations and all our simulations

13

ranges between 4.8 m (GammaI) and 6.5 m (GammaD), and no clear regional patterns can be detected. That is, outside of the southern subpolar gyres, the MLD is not significantly modified by our changes of parameters. It thus seems feasible to reduce Southern Ocean deep convection by tuning these three parameters without impacting the MLD elsewhere.

4 Discussion, limitations and conclusions

We performed sensivity experiments on a global version of NEMO3.4 with prescribed atmospheric forcing to study the trigger of unrealistic Southern Ocean deep convection. A complex chain of events, which preconditioned the ocean, initiated open ocean deep convection in the Riiser-Larsen Sea in winter 1987 in our simulations. It began two years earlier with a weakening of katabatic winds from Antarctica resulting in a negative sea ice anomaly in winter 1985 (Fig. 2a). These results are consistent with those of Goosse and Fichefet (2001) and Kjellsson et al. (2015) that highlight a strong sensitivity of ocean models to sea ice anomalies leading to open ocean deep convection in the Southern Ocean. Note that other ocean models have a similar chain of events and timing, with deep convection in a small area in the Riiser-Larsen Sea triggering a larger event in the central Weddell Sea. The reason why the Riiser-Larsen Sea is so prone to deep convection in ocean models remains an open question to be investigated.

Modifying the oceanic vertical mixing parameters greatly altered the extent of Southern Ocean open ocean deep convection and the process triggering it. The anomaly in sea ice induces anomalies in the top 50 m properties. In agreement with Calvert and Siddorn (2013), we found that the experiments with increased mixing parameters (notably Langmuirl) resulted in smaller surface temperature and salinity anomalies. The perturbed parameter ensemble revealed distinct relationships between the summer and autumn sea surface temperature and the area of the subsequent polynya in winter (Fig. 4). Once the polynya forms, the ocean enters a positive feedback loop: warmer surface leads to larger polynyas, which have more brine rejection and hence lead to deeper convection, which mixes up relatively warm water and leads to even warmer surface waters. A similar process occurs in the

14

Kiel Climate Model (Martin et al., 2013) where winter deep convection persists for decades and reoccurs on centennial timescales. In our simulations, deep convection stops after winter 1987 in the control run and the increased parameter experiments. Longer simulations would be needed to determine if the frequency of occurrence of deep convection is generally diminished. Experiments which reduce the vertical mixing produce strong temperature anomalies, caused by the 1987 event, which are advected westward and result in renewed deep convection across the centre of the Weddell Gyre in 1988 (Fig. 5). These experiments exhibit convection from the surface to the sea bed over most of the Weddell Sea in 1989 when the simulations stop.

Our results are consistent with those of Martin et al. (2013) and Cheon et al. (2014): deep convection increases the ACC volume transport above the range indicated by observations (Fig. 6). Whilst increasing the model vertical mixing dramatically alters the open ocean deep convection in the Southern Ocean, it does not significantly modify the North Atlantic deep convection (Fig. 7). This is the same conclusion reached by Timmermann and Beckmann (2004), although they went to the extent of devising a new vertical mixing scheme specifically for seasonal sea ice regions (which, after correction of a coding error, does not reduce Southern Ocean deep convection, Timmermann and Losch, 2005). Our conclusion is that a similar result can be achieved within the parameterisation of an existing, globally consistent, mixing scheme. Although the parameters changed here are specific to NEMO, increasing vertical mixing in the Southern Ocean in other models is likely to lead to reduced Southern Ocean deep convection, for the mechanism involved would be similar to the ones highlighted in this manuscript. Our results, however, need to be treated with some caution, as our simulations have been too short to determine if the parameter changes result in longer term (i.e. a spun-up model) changes to the mean state of the global ocean simulation. Longer runs would determine the optimum balance between a low-bias global ocean, and a Southern Ocean with reduced deep convection. Longer simulations are also needed to obtain a more appropriate reference period (i.e. after the model has spun up). Further observations would also be beneficial to validate or extend the range of parameter values used in this study, notably LangmuirI.

It is clear that the current state-of-the-art models require Southern Ocean deep convection in order to form their Antarctic Bottom Water (Heuzé et al., 2013). Ideally, they should also represent the actual Weddell Polynya in hindcasts. Hence, open ocean deep convection should be reduced but not totally suppressed. New methods, which focus on shelf overflow parameterisations, are being developed and implemented to form Antarctic Bottom Water in a more physically accurate manner (Snow et al., 2015). Some examples are a pipe from the shelf to the open ocean (Briegleb et al., 2010), porous barriers (Adcroft, 2013) and an embedded Lagrangian model (Bates et al., 2012). By performing a set of vertical mixing sensitivity experiments on the NEMO model, we have shown the general direction that models need to take to at least reduce spurious Southern Ocean deep convection: the vertical mixing needs to be increased, not decreased as one might intuitively think. This paper paves the way for further model improvement that could help ocean models to not form their bottom waters unrealistically, by reducing open ocean deep convection in the southern subpolar gyres.

Author contributions. C. Heuzé and J. K. Ridley designed the experiments and carried them out, following previous results from D. Calvert and with his technical support. D. P. Stevens imported the model output from the Met Office to UEA, and helped with the analysis of results along with K. J. Heywood. C. Heuzé prepared the manuscript with contributions from all co-authors.

Code availability

The model code for NEMO v3.4 is available from the NEMO website (www.nemo-ocean.eu). On registering, individuals can access the FORTRAN code using the open source subversion software (http://subversion.apache.org/). The revision number of the base NEMO code (trunk) used for this paper is 3424. In addition some modifications have been applied to the base code (branches) to create GO5. Please contact Alex Megann (apm@noc.ac.uk) for more information on these branches and how to obtain them. UK users with access to PUMA (cms.ncas.ac.uk/wiki/PumaService) can copy the job details (job ID amhih) and submit a duplicate job using the Met Office Unified Model user interface (UMUI).

References

Adcroft, A.: Representation of topography by porous barriers and objective interpolation of topographic data, Ocean Model., 67, 13–27, doi:10.1016/j.ocemod.2013.03.002, 2013.

Axell, L. B.: Wind-driven internal waves and Langmuir circulations in a numerical ocean model of the southern Baltic Sea, J. Geophys. Res., 107, 3204, doi:10.1029/2001JC000922, 2002.

Azaneu, M., Kerr, R., and Mata, M. M.: Assessment of the representation of Antarctic bottom water properties in the ECCO2 reanalysis, Ocean Sci., 10, 923–946, doi:10.5194/os-10-923-2014, 2014.

Bates, M. L., Griffies, S. M., and England, M. H.: A dynamic, embedded Lagrangian model for ocean climate models. Part I: Theory and implementation, Ocean Model., 59, 51–59, doi:10.5194/os-10-923-2014, 2012.

Briegleb, B. P., Danabasoglu, G., and Large, W.: An overflow parameterization for the ocean component of the community climate system model, Tech. rep, National Center for Atmospheric Research, Boulder, Colorado, 2010.

Calvert, D. and Siddorn, J.: Revised vertical mixing parameters for the UK community standard configuration of the global NEMO ocean model, Tech. rep, Met Office Hadley Centre, 2013.

Cheon, W. G., Park, Y. G., Toggweiler, J. R., and Lee, S. K.: The relationship of Weddell Polynya and open–ocean deep convection to the Southern Hemisphere westerlies, J. Phys. Oceanogr., 44, 694–713, doi:10.1175/JPO-D-13-0112.1, 2014.

Fofonoff, N. P. and Millard, R. C.: Algorithms for computation of fundamental properties of seawater, UNESCO/SCOR/ICES/IAPSO Joint Panel on Oceanographic Tables and Standards, 1983.

Gaspar, P., Grégoris, Y., and Lefevre, J. M.: A simple eddy kinetic energy model for simulations of the oceanic vertical mixing: tests at Station Papa and long–term upper ocean study site, J. Geophys. Res., 95, 16179–16193, doi:10.1029/JC095iC09p16179, 1990.

Goosse, H. and Fichefet, T.: Open-ocean convection and polynya formation in a large-scale ice-ocean model, Tellus A, 53, 94–11, doi:10.1034/j.1600-0870.2001.01061.x, 2001.

Gordon, A. L.: Deep Antarctic convection west of Maud Rise, J. Phys. Oceanogr., 8, 600–612, doi:10.1175/1520-0485(1978)008<0600:DACWOM>2.0.CO;2, 1978.

Griesel, A., Mazloff, M. R., and Gille, S. T.: Mean dynamic topography in the Southern Ocean: evaluating Antarctic circumpolar current transport, J. Geophys. Res., 117, C01020, doi:10.1029/2011JC007573, 2012.

Heuzé, C.: Antarctic Bottom Water in CMIP5 models: Characteristics, Formation, Evolution, Ph.D. thesis, School of Environmental Sciences, University of East Anglia, 2015.

Heuzé, C., Heywood, K. J., Stevens, D. P., and Ridley, J. K.: Southern Ocean bottom water characteristics in CMIP5 models, Geophys. Res. Lett., 40, 1409–1414, doi:10.1002/grl.50287, 2013.

Heuzé, C., Heywood, K. J., Stevens, D. P., and Ridley, J. K.: Changes in global ocean bottom properties and volume transports in CMIP5 models under climate change scenarios, J. Climate, online first, doi:10.1175/JCLI-D-14-00381.1, 2015.

Hunke, E. C. and Lipscomb, W. H.: CICE: the Los Alamos Sea Ice Model Documentation and Software User's Manual Version 4.0, Los Alamos National Laboratory, 2008.

Johnson, G. C.: Quantifying Antarctic bottom water and North Atlantic deep water volumes, J. Geophys. Res., 113, C05027, doi:10.1029/2007JC004477, 2008.

Killworth, P. D.: On "chimney" formations in the ocean, J. Phys. Oceanogr., 9, 531–554, doi:10.1175/1520-0485(1979)009<0531:OFITO>2.0.CO;2, 1979.

Kjellsson, J, Holland, P. R., Marshall, G. J., Mathiot, P., Aksenov, Y., Coward, A. C., Bacon, S., Megann, A. P., and Ridley, J. K.: Model sensitivity of the Weddell and Ross seas, Antarctica, to vertical mixing and freshwater forcing, Ocean Model., 94, 141–152, doi:10.1016/j.ocemod.2015.08.003, 2015.

Large, W. G. and Yeager, S. G.: The global climatology of an interannually varying air–sea flux data set, Clim. Dynam., 33, 341–364, doi:10.1007/s00382-008-0441-3, 2009.

Latif, M., Martin, T., and Park, W.: Southern Ocean sector centennial climate variability and recent decadal trends, J. Climate, 26, 7767–7782, doi:10.1175/JCLI-D-12-00281.1, 2013.

Li, M. and Garrett, C.: Cell merging and the jet/downwelling ratio in Langmuir circulation, J. Mar. Res., 51, 737–769, doi:10.1357/0022240933223945, 1993.

Losch, M., Herlufsen, S., and Timmermann, R.: Effects of heterogeneous surface boundary conditions on parameterized oceanic deep convection, Ocean Model., 13, 156–165, doi:10.1016/j.ocemod.2005.12.003, 2006.

Madec, G.: NEMO ocean general circulation model reference manuel, Tech. rep, LOCEAN/IPSL, Paris, 2008.

Martin, T., Park, W., and Latif, M.: Multi–centennial variability controlled by Southern Ocean convection in the Kiel climate model, Clim. Dynam., 40, 2005–2022, doi:10.1007/s00382-012-1586-7, 2013.

Martin, T., Park, W., and Latif, M.: Southern Ocean Forcing of the North Atlantic at Multi-centennial Time Scales in the Kiel Climate Model, Deep Sea Res. Part II, 114, 39–48, doi:10.1016/j.dsr2.2014.01.018, 2015.

Martinson, D. G., Killworth, P. D., and Gordon, A. L.: A convective model for the Weddell Polynya, J. Phys. Oceanogr., 11, 466–488, doi:10.1175/1520-0485(1981)011<0466:ACMFTW>2.0.CO;2, 1981.

Megann, A., Storkey, D., Aksenov, Y., Alderson, S., Calvert, D., Graham, T., Hyder, P., Siddorn, J., and Sinha, B.: GO5.0: the joint NERC–Met Office NEMO global ocean model for use in coupled and forced applications, Geosci. Model Dev., 7, 1069–1092, doi:10.5194/gmd-7-1069-2014, 2014.

Meijers, A. J. S., Shuckburgh, E., Bruneau, N., Sallée, J.-B., Bracegirdle, T. J., and Wang, Z.: Representation of the Antarctic Circumpolar Current in the CMIP5 climate models and future changes under warming scenarios, J. Geophys. Res., 117, C12008, doi:10.1029/2012JC008412, 2012.

Rodgers, K. B., Aumont, O., Mikaloff Fletcher, S. E., Plancherel, Y., Bopp, L., de Boyer Montégut, C., Iudicone, D., Keeling, R. F., Madec, G., and Wanninkhof, R.: Strong sensitivity of Southern Ocean carbon uptake and nutrient cycling to wind stirring, Biogeosciences, 11, 4077–4098, doi:10.5194/bg-11-4077-2014, 2014.

Russell, J. L., Stouffer, R. J., and Dixon, K. W.: Intercomparison of the Southern Ocean circulations in IPCC coupled model control simulations, J. Climate, 19, 4060–4075, doi:10.1175/JCLI3869.1, 2006.

Schmidtko, S., Johnson, G. C., and Lyman, J. M.: MIMOC: A global monthly isopycnal upper–ocean climatology with mixed layers, J. Geophys. Res., 118, 1658–1672, doi:10.1002/jgrc.20122, 2013.

Shaffrey, L. C., Stevens, I., Norton, W. A., Roberts, M. J., Vidale, P. L., Harle, J. D., Jrrar, A., Stevens, D. P., Woodage, M. J., Demory, M. E., Donners, J., Clark, D. B., Clayton, A., Cole, J. W., Wilson, S. S., Connolley, W. M., Davies, T. M., Iwi, A. M., Johns, T. C., King, J. C., New, A. L., Slingo, J. M., Slingo, A., Steenman-Clark, L., and Martin, G. M.: U.K. HiGEM: The new U.K. high-

resolution global environment model – model description and basic evaluation, J. Climate, 22, 1861–1896, doi:10.1175/2008JCLI2508.1, 2009.

Snow, K., Hogg, A., Downes, S. M., Sloyan, B. M., Bates, M. L., and Griffies, S. M.: Sensitivity of abyssal water masses to overflow parameterisations, Ocean Model., 89, 84–103, doi:10.1016/j.ocemod.2015.03.004, 2015.

Smith, W. O. and Barber, D.: Polynyas: Windows to the World, Elsevier, Amsterdam, 2007.

Timmermann, R. and Losch, M.: Using the Mellor–Yamada mixing scheme in seasonally ice-covered seas – Corrigendum to: Parameterization of vertical mixing in the Weddell Sea [Ocean Modelling 6 (2004) 83–100], Ocean Model., 10, 3–4, doi:10.1016/j.ocemod.2004.11.001, 2005.

Timmermann, R. and Beckmann, A.: Parameterization of vertical mixing in the Weddell Sea, Ocean Model., 6, 83–100, doi:10.1016/S1463-5003(02)00061-6, 2004.

Våge, K., Pickart, R. S., Thierry, V., Reverdin, G., Lee, C. M., Petrie, B., Agnew, T. A., Wong, A., and Ribergaard, M. H.: Surprising return of deep convection to the subpolar North Atlantic ocean in winter 2007–2008, Nat. Geosci., 2, 67–72, doi:10.1038/ngeo382, 2009.

Table 1. Sensitivity experiments performed on NEMO3.4, detailed in Sect. 2: "Langmuir" experiments look at Langmuir turbulence velocity scale, "Gamma" at the penetration of an additional turbulent kinetic energy term below the mixed layer, "Knoprof" and "KProf" at background diffusivity. "I" indicates that the parameter was increased compared to the reference value, "D" that it was decreased. The parameters column identifies the shorthand name used in the NEMO simulation name-list. Note that the "Control" run is 10 years long.

| name	parameter	value	value in 'Control'	run length
LangmuirD	ln_lc	false	true	10 yr
LangmuirI	rn_lc	0.20	0.15	10 yr
GammaD	rn_efr	0.005	0.05	10 yr
GammaI	rn_efr	0.095	0.05	10 yr
KnoProfD	rn_avt0	1.0×10^{-5}	1.2×10^{-5}	27 yr
KProf	nn_avb	1	0	27 yr
KProfI	nn_avb	1	0	27 yr
	rn_avt0	1.3×10^{-5}	1.2×10^{-5}	
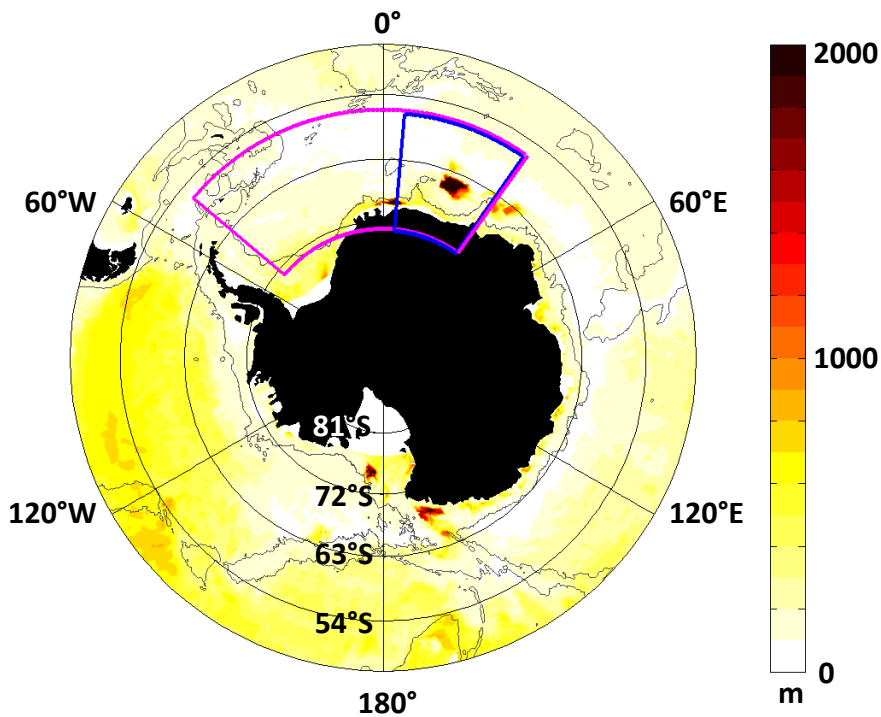
Figure 1. NEMO3.4, control run, for each grid point, maximum monthly mixed layer depth between January 1980 and December 1989. The blue box indicates the Riiser-Larsen Sea region, which is overlaid by the magenta box that indicates the Weddell Sea region studied in Sect. 3.2.
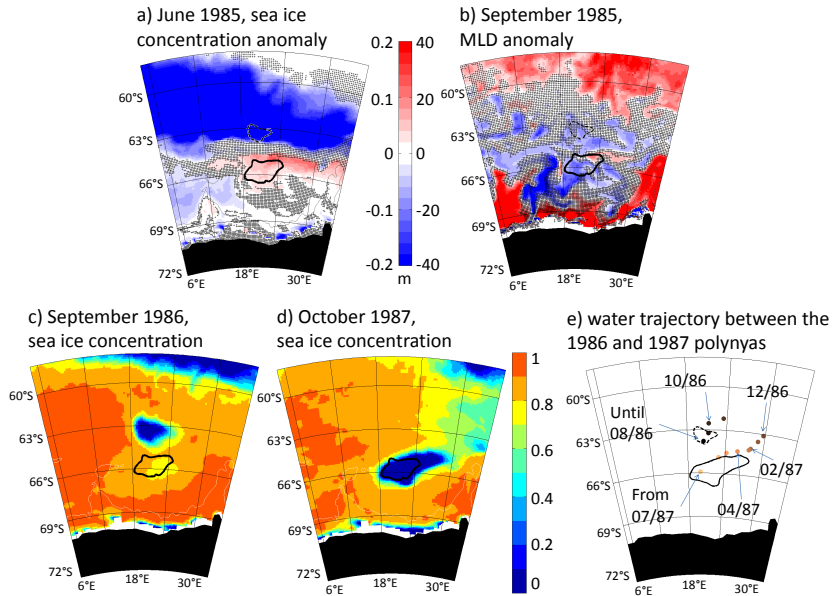
Figure 2. Chain of events leading to deep convection in 1987: a) sea ice concentration anomaly in June 1985; b) MLD anomaly in September 1985; c) and d) sea ice concentration in September 1986 and October 1987; e) trajectory of the water between the two polynyas of 1986 (dashed black line) and 1987 (continuous black line, see text). Stippling on a) and b) indicates areas where the anomalies are not significant. Dashed contours on a) and b) indicates the location of the 1986 polynya. Black contours on a) to d) indicate the area where the maximum MLD from Fig. 1 exceeds 2000 m, while grey contours indicate the 3000 m isobath.
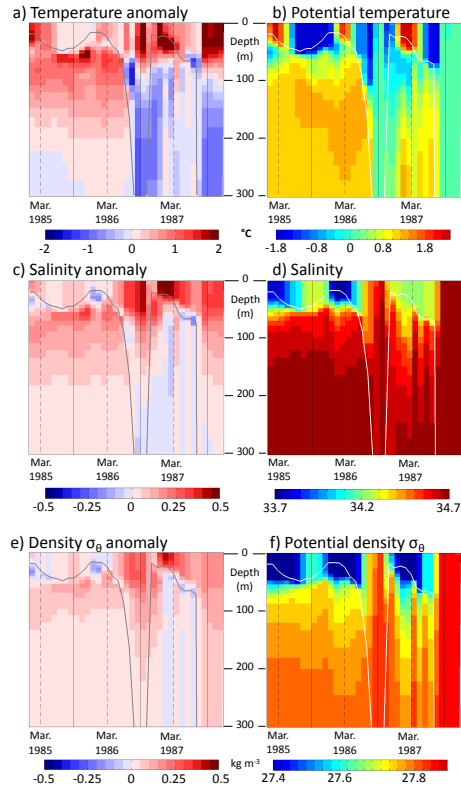
Figure 3. Hovmoller diagrams, as a function of depth and time, of properties averaged over the area of the 1986 polynya (dashed black contour on Fig. 2e) until August 1986, along the trajectory of Fig. 2e from September 1986 to June 1987, and over the area of the 1987 polynya (plain black contour on Fig. 2e) from July 1987: a) potential temperature anomalies (relative to Jan. 1980 to Dec. 1984); b) potential temperature; c) salinity anomaly (relative to Jan. 1980 to Dec. 1984); d) salinity; e) potential density σ_θ anomaly (relative to Jan. 1980 to Dec. 1984); f) potential density σ_θ. Grey line on a), c) and e) and white line on b), d) and f) is the MLD.
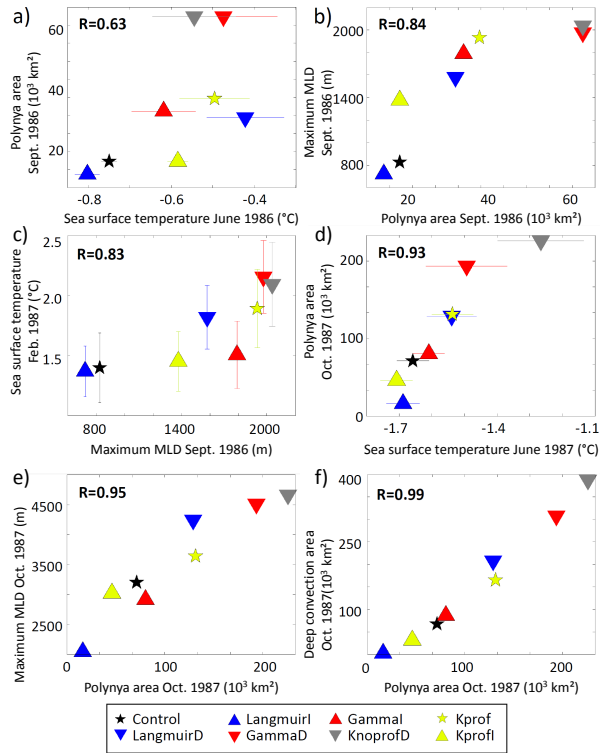
Figure 4. Across-run significant relationships between the steps leading to the deep convection event of winter 1987. **(a)** Sea surface temperature in June 1986 and polynya area in September 1986; **(b)** polynya area and maximum depth of the mixed layer, both in September 1986; **(c)** maximum depth of the mixed layer in September 1986 and sea surface temperature in February 1987; **(d)** sea surface temperature in June 1987 and polynya area in October 1987; **(e)** polynya area and maximum depth of the mixed layer, both in October 1987; **(f)** polynya area and deep convection area, both in October 1987. Horizontal bars on a) and d) and vertical bars on c) indicate the standard deviation relative to spatial variability.
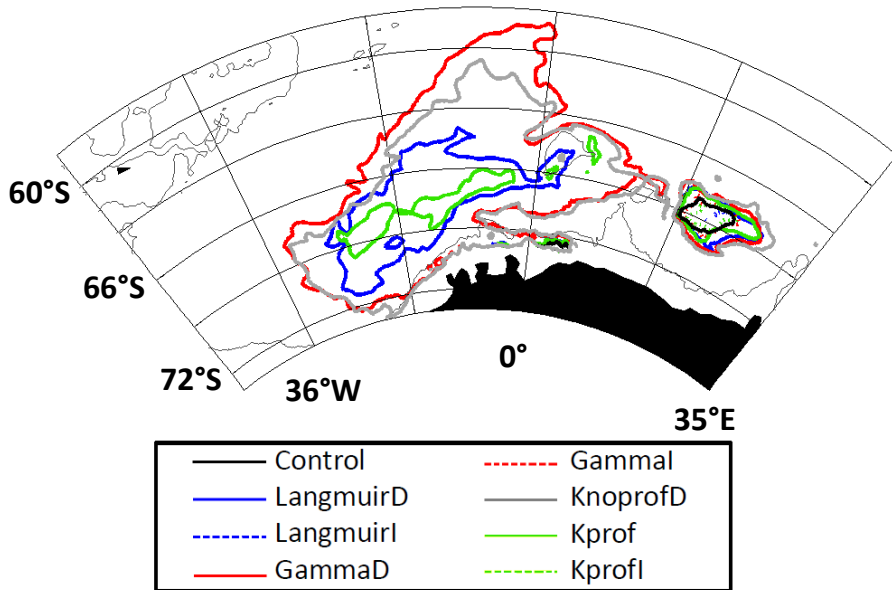
Figure 5. For each experiment, contours indicating where the maximum 1980–1989 MLD exceeds 2000 m in the Weddell Gyre region (magenta box in Fig. 1). Thin grey contours indicate the 3000 m isobath. Note that the contours for the increased-parameter experiments and the control mostly coincide.
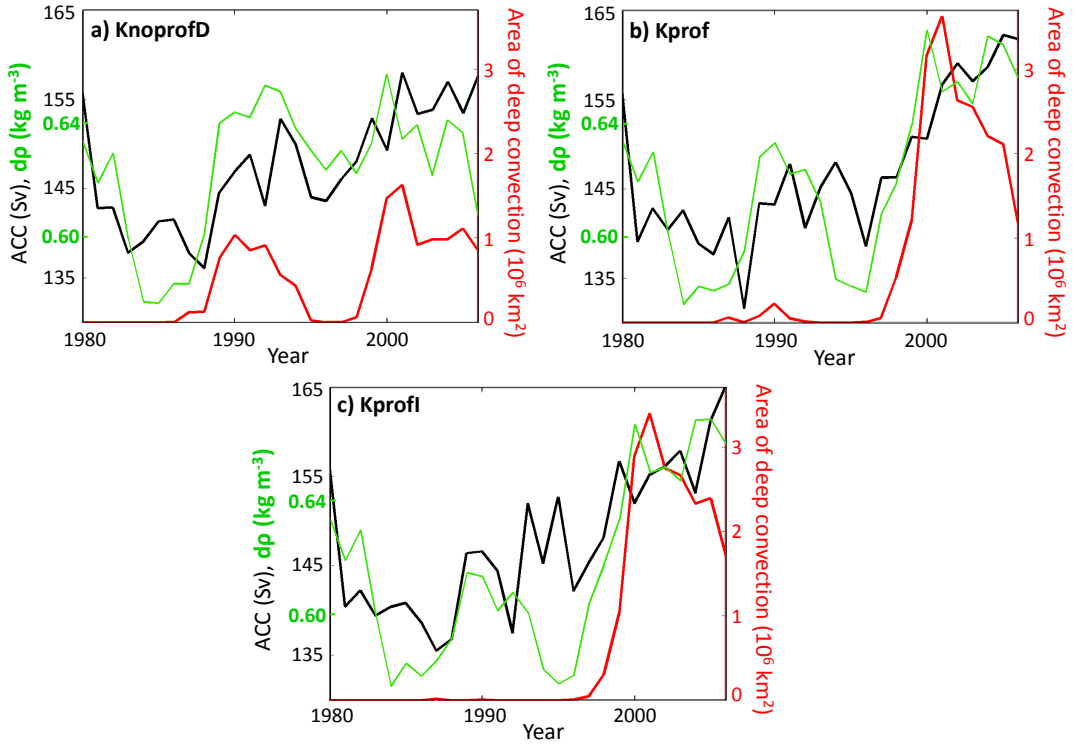
Figure 6. 27-year time series of the annual maximum ACC (black), annual mean horizontal gradient in density $d\rho$ (green) and annual maximum area of deep convection in the Southern Ocean (red).
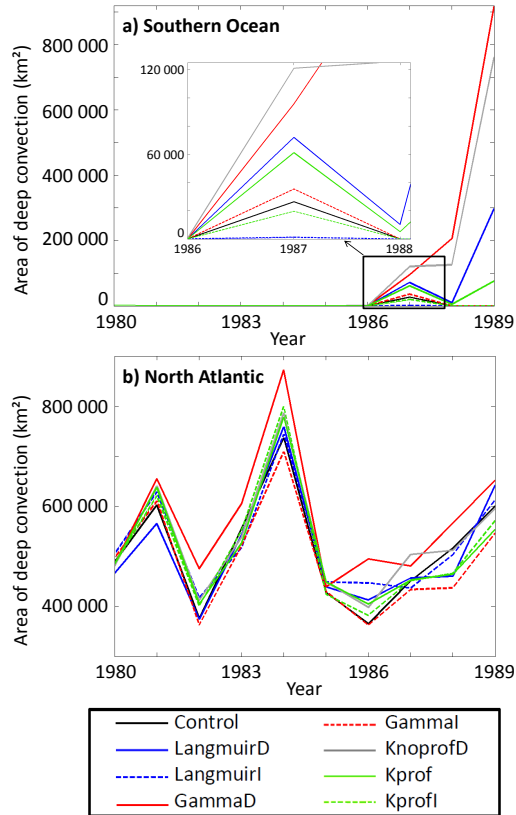
Figure 7. For each experiment, annual maximum area of deep convection in **(a)** the Southern Ocean and **(b)** the North Atlantic.